Khalifa, Hany; Jäntti, Riku

Retrieving quantum backscattered signals in the presence of noise

Published in:
2019 IEEE Globecom Workshops, GC Wkshps 2019 - Proceedings

DOI:
10.1109/GCWkshps45667.2019.9024525

Published: 01/12/2019

Document Version
Peer reviewed version

Please cite the original version:
Khalifa, H., & Jäntti, R. (2019). Retrieving quantum backscattered signals in the presence of noise. In *2019 IEEE Globecom Workshops, GC Wkshps 2019 - Proceedings* [9024525] IEEE.
https://doi.org/10.1109/GCWkshps45667.2019.9024525

Retrieving quantum backscattered signals in the presence of noise

Hany Khalifa* and Riku Jäntti
Aalto University, Department of Communications and Networking, Espoo, 02150, Finland

Quantum sensing based on entangled photon pairs is gradually establishing itself as a cornerstone in modern communication networks. The unrivalled capability of quantum sensing techniques in distilling signals plagued by noise, renders them suitable for deployment in backscatter communication networks. Several attempts have been made recently to utilize pairs of entangled signal-idler photons, to enhance the sensitivity of photo-detection in backscatter networks. However, these efforts have always assumed the lossless retention of the idler mode, which is a challenging task from a practical perspective. In this study we examine the extent to which quantum correlations remain after retaining the idler mode in a lossy memory element, while the signal photon propagates through a lossy thermal channel as usual. We also examine briefly two different detection methods, and estimate the received signal-to-noise ratio for them both. This new proposed model is one step further towards realizing quantum backscatter communication.

I. Introduction

Metrology is more or less the branch of science concerned with devising efficient detection schemes, in order to reliably retrieve modulated information. Owing to the impetus given to the sensor industry by its ability to perform super-resolution measurements, quantum sensing [1] is nowadays reckoned as the next evolutionary step towards enhanced metrology for quantum communication systems. The workhorse of almost all quantum-enhanced protocols is quantum entanglement. Quantum entnaglement [2] is characterized by its inimitable non-local correlations that can be sustained, at least theoretically, over large distances. In the past few decades, numerous protocols which derive benefit from entanglement as a resource have been proposed in both the optical and microwave domains. In the optical domain, secure quantum communication [3, 4], satellite quantum key distribution [5, 6], quantum teleportation [7, 8], noiseless linear amplifiers [9], and quantum repeaters[10] have been experimentally demonstrated with both continuous variables (CV) and photon number states.

On the other hand, microwave quantum technologies rely on the use of superconducting elements as their comprising components, which are only operable inside cryogenic environments. Thus, advances in this doamin are mainly theoretical [11]. Notable efforts have been made in the field of microwave quantum communication, the most renowned among them are microwave quantum teleportation [12] and quantum illumination enhanced sensing [13, 14].

In this paper we will focus on a new application in which quantum approaches can be used for improved sensitivities and resolutions, namely, quantum backscatter communication (QBC) [15–17]. Quantum backscattering is a branch of quantum communication, which exploits quantum entanglement in order to distil backscattered signals propagating through a noisy thermal channel. In a typical QBC scenario, a tag antenna communicates classical information (identification number) to an interrogator by either reflecting or not reflecting a probe signal sent by the interrogator. The aforementioned simple modulation technique can be accurately modelled by a lossless quantum beamsplitter [18]. Unlike its classical analogue, the quantum beamsplitter mixes a single input with vacuum noise entering from its unused dark port. Thus, the tag antenna can be treated as a 2 port network having 2 inputs and 2 outputs. This abstract description of the QBC system is extremely flexible, such that its realization is not restricted to one particular frequency range. Optical realizations are favoured when open air quantum communication is considered [11], since at room temperature the number of noise photons is $\ll 1$. On the contrary, microwave superconducting circuits do not function properly at room temperature, since in the 2-7 GHz range—the typical operating point of such devices— the number of black body photons is in the vicinity of 10^3. As a consequence, realizations in the microwave domain will always find themselves enthralled within cryogenic structures. Nevertheless, this exceptionally intricate environment is sufficient for quantum computing applications. Moreover, since the tag antenna can be regarded abstractly as a beamsplitter, which in the context of quantum computing realizes a phase gate [18], we can fit our QBC model within a framework for an all-linear microwave quantum computer, in a manner that imitates its renowned optical analogue [19]. Linear optical quantum computing showed great scalability and ease of implementation, where its proposed scheme only utilises beam splitters, phase shifters, single photon sources and photo-detectors. Alongside microwave beamsplitters, low power backscatter devices employed as phase gates, could pave the way for scalable and efficient linear microwave quantum computing.

Recently, a few prototypes have been proposed for realizing quantum backscattering with both continuous variables and photon number states [15–17]. The main theme of these approaches was the lossless possession of the idler mode throughout the duration of the whole protocol. In our new model we release this demanding assumption by storing the idler mode in a lossy memory element. In other words, we will assume that the idler mode propagates through a pure loss channel until a measurement is performed. We believe that this new model is more practical and realistic.

In the next few sections we study thoroughly the effect of this new assumption on the correlations between the signal and idler photons, and show that quantum backscattering can be achieved under this new consideration.

This paper is organized as follows. In section II we describe the effect of propagation losses on quantum correlations in QBC systems. Section III investigates the signal-to-noise ratio at the receiver. Finally, section IV will be our conclusion.

*Electronic address: hany.khalifa@aalto.fi

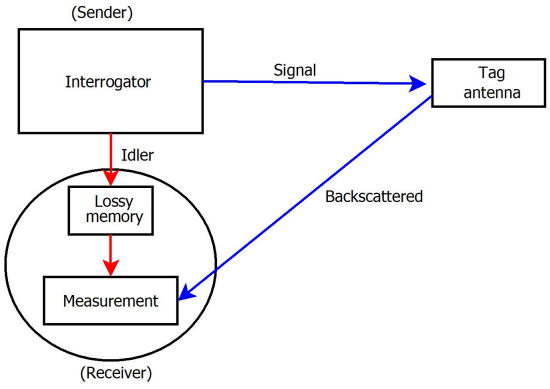

FIG. 1: *QBC block diagram*

II. Backscattering with Gaussian entangled states

A. Quantum backscatter communication (QBC)

The aim of QBC is to capture faint signals backscattered by a tag antenna, which is embedded in a noisy thermal environment. As depicted in Fig.1, the sender is a photon source that generates entangled photon pairs. The mode A (signal) is transmitted to probe a tag antenna immersed in a heat bath. The mode B (idler) is retained at the receiver—which is co-located with the transmitter— to be measured with the backscattered mode A.

We will assume that the retention process is carried out by a memory element that can be modelled accurately by a pure loss channel. This new treatment is a little bit different from earlier ones [15–17], where the idler mode was assumed to be retained losslessly at the receiver. The tag antenna can be modelled by a low reflectivity beamsplitter, where thermal noise enters from the beamsplitter's dark port. In a quintessential QBC scenario, the tag antenna switches between two states denoted transmitting (on) and non-transmitting (off). During the "on" state the backscattered signal is mixed with thermal noise, while in the "off" state only thermal noise enters the receiver:

$$\begin{aligned} &\textbf{Transmitting (on)} : \hat{\rho}_{\text{on}} = \text{Tr}_{\text{Th}}[\hat{U}(\hat{\rho}_{\text{AB}} \otimes \hat{\rho}_{\text{Th}})\hat{U}^{\dagger}] \\ &\textbf{Non-transmitting (off)} : \hat{\rho}_{\text{off}} = \text{Tr}_{\text{A}}[\hat{\rho}_{\text{AB}}] \otimes \hat{\rho}_{\text{Th}} \end{aligned} \tag{1}$$

where $\hat{U}$ is a completely positive trace preserving map (CPTP), $\hat{\rho}_{\text{AB}}$ is the signal-idler joint density operator, $\hat{\rho}_{\text{Th}}$ is the thermal state of the environment and "Tr" is the partial trace operation.

B. Entanglement of a two mode squeezed state [20]

Quantum entanglement is indispensable for the operation of QBC. Entangled two-mode squeezed states (TMSS) have proven to be most popular, owing to their ease of production and versatility. Thus, TMSS are extensively used in almost every entanglement-based communication protocol. In the number basis a TMSS is written as:

$$|\text{TMSS}\rangle = \sqrt{1-\lambda^2}\sum_{\text{n}=0}^{\infty}\lambda^n\,|\text{n}\rangle\,|\text{n}\rangle \tag{2}$$

where $\lambda = \tanh \text{r}$, and r is the squeezing parameter. At the transmitter a TMSS is generated by the process of spontaneous parametric down conversion (SPDC) [18], where a strong laser pump is disintegrated into a pair of signal & idler photons. The signal is sent to probe the tag antenna, while the idler is retained in a lossy memory element at the receiver.

Entanglement of a Gaussian TMSS is quantified by its covariance matrix, where it can be written in terms of the quadrature operators $\hat{\text{x}}_{\text{a}}, \hat{\text{p}}_{\text{a}}, \hat{\text{x}}_{\text{b}}, \hat{\text{p}}_{\text{b}}$ defined as $\hat{\text{x}}_{\text{k}} = (\hat{\text{a}}_{\text{k}} + \hat{\text{a}}_{\text{k}}^{\dagger})/\sqrt{2}$, $\hat{\text{p}}_{\text{k}} = (\hat{\text{a}}_{\text{k}} - \hat{\text{a}}_{\text{k}}^{\dagger})/\text{i}\sqrt{2}$, where k = a,b. Furthermore, we can arrange these operators in the following row vector $\hat{\mathbf{X}} = (\hat{\text{x}}_{\text{a}}, \hat{\text{p}}_{\text{a}}, \hat{\text{x}}_{\text{b}}, \hat{\text{p}}_{\text{b}})$, as a consequence, the covariance matrix can be written as

$$\mathbf{CV}_{\text{kl}} = \frac{\mathbf{1}}{\mathbf{2}}\langle \hat{\mathbf{X}}_{\text{k}}\hat{\mathbf{X}}_{\text{l}} + \hat{\mathbf{X}}_{\text{l}}\hat{\mathbf{X}}_{\text{k}}\rangle - \langle \hat{\mathbf{X}}_{\text{k}}\rangle\langle \hat{\mathbf{X}}_{\text{l}}\rangle \tag{3}$$

where k,l = a,b, $\hat{\mathbf{X}}_{\mathbf{a}} = (\hat{\text{x}}_{\text{a}}, \hat{\text{p}}_{\text{a}})$ and $\hat{\mathbf{X}}_{\mathbf{b}} = (\hat{\text{x}}_{\text{b}}, \hat{\text{p}}_{\text{b}})$

In the context of QBC, the covariance matrix can be written in the following block form

$$\mathbf{CV} = \begin{pmatrix} \alpha & \gamma \\ \gamma^T & \beta \end{pmatrix}. \tag{4}$$

The eigenvalues of the block covariance matrix (known also as the symplectic spectrum), determine whether a Gaussian TMSS is entangled or not. The symplectic eigenvalues $\nu_{\pm}$ are defined as

$$\nu_{\pm} = \sqrt{\frac{1}{2}\Big(\Delta \pm \sqrt{\Delta^2 - 4\det \mathbf{CV}}\Big)}\,, \tag{5}$$

where $\det \mathbf{CV}$ is the determinant of the covariance matrix and

$$\Delta = \det\alpha + \det\beta - 2\det\gamma \tag{6}$$

For an entangled state, the smallest of the two symplectic eigenvalues ν_{-} is always $< 1/2$ and the violation of this condition implies that the state is separable.

C. Survival of quantum correlations in lossy media

As highlighted earlier, the generated signal and idler modes will propagate through a heat bath and a pure loss channel respectively. Due to their interaction with the environment, both modes will suffer significant loss. Thus, our task in this section is to investigate the survivability of the signal-idler entanglement under these two loss mechanisms. The losses accompanying a mode propagating through a thermal channel are exactly similar to those experienced by a damped simple harmonic oscillator (SHO). Thus, the dynamical equations which describe the interaction between a SHO and a heat bath (environment) can model our problem precisely [18]. To describe the damping of a SHO, one has to derive first the field's master equation, then utilizes it to calculate the decay rate of the mode operator (see appendix A 1). Fortunatley, this complicated process can be captured accurtely by a beamsplitter model [18].

We begin now our analysis by first considering the signal mode. After traversing the thermal channel, the mode operator is given by

$$\hat{\mathbf{a}}_{\mathbf{signal,out}} = \mathbf{\Gamma}_{\mathbf{signal}}\hat{\mathbf{a}}_{\mathbf{signal,in}} + \hat{\mathbf{N}}_{\mathbf{signal}} \tag{7}$$

where $\hat{\mathbf{a}}_{\mathbf{signal,out}}$ is the channel's output, $\hat{\mathbf{a}}_{\mathbf{signal,in}}$ is its input, $\mathbf{\Gamma}_{\mathbf{signal}}$ is the channel's transmission efficiency and $\hat{\mathbf{N}}_{\mathbf{signal}}$ is a fluctuating noise term.

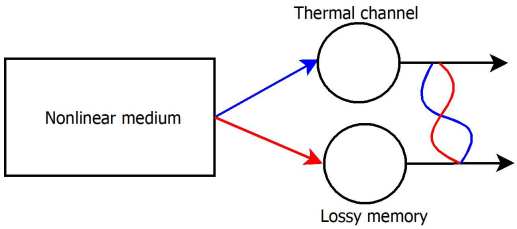

FIG. 2: *Two-mode entangled Gaussian state in lossy media.*

The fluctuating Langevin force $\hat{\mathbf{N}}$ was added to the mode operator input-output equation, in order that the commutation relation for the output mode is preserved.

$$[\hat{\mathbf{a}}_{\mathbf{signal,out}}, \hat{\mathbf{a}}^{\dagger}_{\mathbf{signal,out}}] = [\hat{\mathbf{a}}_{\mathbf{signal,in}}, \hat{\mathbf{a}}^{\dagger}_{\mathbf{signal,in}}] = \mathbf{1} \tag{8}$$

The noise properties of the thermal bath are

$$\begin{aligned} [\hat{\mathbf{N}}, \hat{\mathbf{N}}^{\dagger}]_{\mathbf{signal}} &= \mathbf{1} - \mathbf{\Gamma}^{\mathbf{2}}_{\mathbf{signal}} \\ \langle \hat{\mathbf{N}}^{\dagger} \hat{\mathbf{N}} \rangle_{\mathbf{signal}} &= \bar{\mathbf{n}} \end{aligned} \tag{9}$$

where $\bar{\mathbf{n}}$ is the average number of black body photons in a thermal bath $\left[\exp(\frac{-\hbar\omega}{\mathbf{k_b T}})\left[\mathbf{1} - \exp(\frac{-\hbar\omega}{\mathbf{k_b T}})\right]^{-\mathbf{1}}\right]$, $\hbar$ is Planck's constant, ω is the mode frequency, $\mathbf{k}_\mathrm{b}$ is Boltzmann's constant and $\mathbf{T}$ is the bath temperature.
On the other hand, the lossy memory element, where the idler mode is kept, is modelled by a pure loss channel [21, 22], i.e. a bath at zero temperature. The output mode operator after propagating through that channel will be

$$\hat{\mathbf{a}}_{\mathbf{idler,out}} = \mathbf{\Gamma}_{\mathbf{idler}} \hat{\mathbf{a}}_{\mathbf{idler,in}} + \hat{\mathbf{N}}_{\mathbf{idler}} \tag{10}$$

For simplicity, we assumed that both channels have the same transmission efficiency $\mathbf{\Gamma}$— this assumption will not affect any future calculations— nonetheless, their noise properties are radically different

$$\begin{aligned} [\hat{\mathbf{N}}, \hat{\mathbf{N}}^{\dagger}]_{\mathbf{idler}} &= \mathbf{1} - \mathbf{\Gamma}^{\mathbf{2}}_{\mathbf{idler}} \\ \langle \hat{\mathbf{N}}^{\dagger} \hat{\mathbf{N}} \rangle_{\mathbf{idler}} &= \mathbf{0} \end{aligned} \tag{11}$$

Now we are ready to calculate the covariance matrix in (3). As shown in Fig.2 the down-converter produces TMSS that can be described as

$$|\zeta\rangle = \exp(\zeta \hat{\mathbf{a}}^{\dagger}_{\mathbf{signal}} \hat{\mathbf{a}}^{\dagger}_{\mathbf{idler}} - \zeta^{*} \hat{\mathbf{a}}_{\mathbf{signal}} \hat{\mathbf{a}}_{\mathbf{idler}}) \, |\mathbf{0}, \mathbf{0}\rangle_{\mathbf{vac}} \tag{12}$$

where $\hat{\mathcal{S}}(\zeta) = \exp(\zeta \hat{\mathbf{a}}^{\dagger}_{\mathbf{signal}} \hat{\mathbf{a}}^{\dagger}_{\mathbf{idler}} - \zeta^{*} \hat{\mathbf{a}}_{\mathbf{signal}} \hat{\mathbf{a}}_{\mathbf{idler}})$ is the two-mode squeezing operator, and $\zeta = \mathbf{r} e^{i\phi}$ is the squeezing parameter w.r.t some phase offset. The covariance matrix now can be written as (see also appendix A 3)

$$\begin{aligned} \mathbf{CV}_{\mathrm{si}} = \frac{\mathbf{1}}{\mathbf{2}} &\langle \mathbf{0}, \mathbf{0} | \, \hat{\mathcal{S}}^{\dagger}(\zeta) (\hat{\mathbf{X}}_{\mathrm{s}} \hat{\mathbf{X}}_{\mathrm{i}} + \hat{\mathbf{X}}_{\mathrm{i}} \hat{\mathbf{X}}_{\mathrm{s}}) \hat{\mathcal{S}}(\zeta) \, | \mathbf{0}, \mathbf{0} \rangle \\ &- \langle \mathbf{0}, \mathbf{0} | \, \hat{\mathcal{S}}^{\dagger}(\zeta) \hat{\mathbf{X}}_{\mathrm{s}} \hat{\mathcal{S}}(\zeta) \, | \mathbf{0}, \mathbf{0} \rangle \, \langle \mathbf{0}, \mathbf{0} | \, \hat{\mathcal{S}}^{\dagger}(\zeta) \hat{\mathbf{X}}_{\mathrm{i}} \hat{\mathcal{S}}(\zeta) \, | \mathbf{0}, \mathbf{0} \rangle \end{aligned} \tag{13}$$

where s, i denote signal and idler respectively. Now since each mode is subjected individually to its respective loss mechanism, the quadrature operators $\hat{\mathbf{X}}_{\mathbf{s}}$, $\hat{\mathbf{X}}_{\mathbf{i}}$ will be expressed in terms of (7) and (10), alongside their accompanying noise properties.

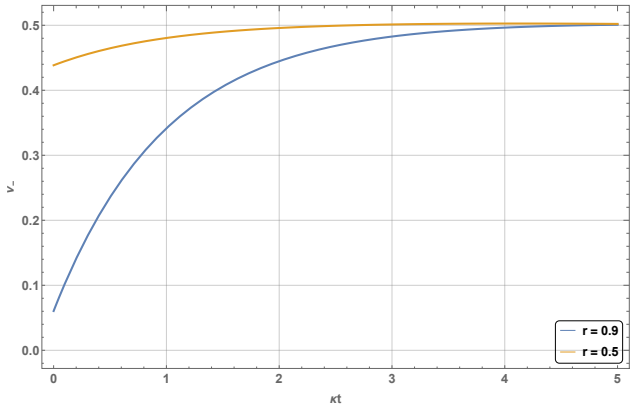

FIG. 3: *Sudden-death of entanglement in a thermal environment plotted for different values of the squeezing parameter.*

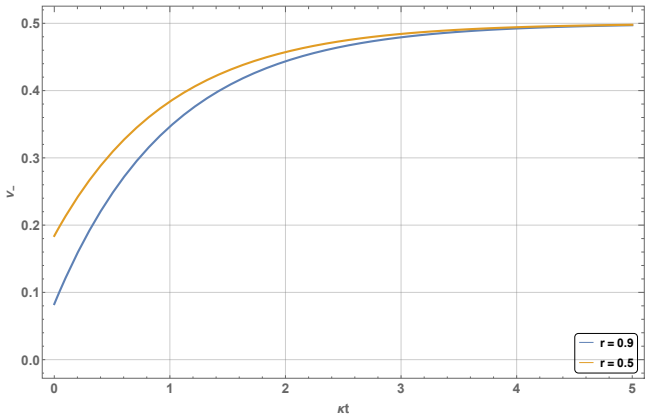

FIG. 4: *Entanglement is preserved when each mode propagates through a pure loss channel.*

Therefore, the block elements of the covariance matrix in (4) will be

$$\alpha = \begin{pmatrix} \mathbf{a} & \mathbf{0} \\ \mathbf{0} & \mathbf{a} \end{pmatrix}. \tag{14}$$

$$\beta = \begin{pmatrix} \mathbf{b} & \mathbf{0} \\ \mathbf{0} & \mathbf{b} \end{pmatrix}. \tag{15}$$

$$\gamma = \gamma^{\mathrm{T}} = \begin{pmatrix} -\mathbf{c} & \mathbf{0} \\ \mathbf{0} & \mathbf{c} \end{pmatrix}. \tag{16}$$

where $\mathbf{a} = (\mathbf{e}^{-\mathbf{2}\kappa\mathbf{t}} \sinh^{\mathbf{2}} \mathbf{r}) + \mathbf{1/2}$, $\mathbf{b} = (\mathbf{e}^{-\mathbf{2}\kappa\mathbf{t}} \sinh^{\mathbf{2}} \mathbf{r}) + \mathbf{1/2} + \bar{\mathbf{n}}$, $\mathbf{c} = (\mathbf{1/2}) \mathbf{e}^{-\mathbf{2}\kappa\mathbf{t}} \sinh \mathbf{2r}$.
In order to highlight the physics behind the damping of a SHO, we redefined the channel's transmission efficiency Γ as a time dependent decay rate, such that κ is its damping constant. This new definition is more suited to our model, since memory leaks are best described as time-dependent processes. The lossy memory element can be a leaky cavity, a fiber loop, or a lossy transmission line.
Thus, by using (5) we can calculate the smallest symplectic eigenvalue and examine whether the original TMSS remains entangled or not. To make our analysis look more complete,

we have plotted the smallest symplectic eigenvalue ν_- against the decay rate κt. As can be seen in Fig.3 the entanglement criterion is violated as soon as $\bar{\mathbf{n}}$ becomes non-zero, thus the effect of the interaction with the heat bath is to break the entanglement between the signal and idler modes. This phenomenon is also know as entanglement sudden death [23].
One way to get around this problem is to decompose the channel into a cascade of n channels, where each introduces $\bar{\mathbf{n}} \ll 1$ noise photons. Nonetheless, in such case, the overall decay rate will be accelerated $\mathbf{e^{-n\kappa t}}$. Similar approaches can also be found in the literature under the name "Bath engineering" [24], where several techniques have been developed to increase the temperature of the environment adiabatically. Our own solution to the problem of entnaglement sudden-death is demonstrated in appendix A 2. We have considered also another interesting case, where each mode decays according to (10) with the same decay constant κ. As shown in Fig.4, the symplectic eigenvalue ν_- is always $< 1/2$ and hence the entanglement between the two modes survives as the entangled light propagates through a pure loss channel [22].
This result is of particular interest, especially when we deploy the QBC model in the context of quantum computing, since it shows that entanglement can withstand passive coupling losses.

III. signal-to-noise ratio considerations [25]

As discussed earlier, entangled states are fragile and can decay rapidly to a statistical mixture of states through their interaction with the environment. Thus, we will consider the effect of transmission losses on the received signal-to-noise ratio (SNR), in order to estimate the number of signal-idler pairs that can survive travelling over a noisy and lossy channel.
The adopted detection method will decide which SNR expression is more suitable. For direct detection (photon counting), the SNR is defined as

$$\mathbf{SNR} = \frac{\langle \hat{\mathbf{n}} \rangle^2}{\langle \Delta \hat{\mathbf{n}}^2 \rangle} \tag{17}$$

where $\hat{\mathbf{n}}$ is the photon number operator.
While for quadrature measurement the same expression can not be used, since $\langle \hat{\mathbf{X}} \rangle = \mathbf{0}$. Thus, we have to redefine the SNR in terms of the variance of the quadrature operator [26].

$$\mathbf{SNR} = \frac{\mathbf{Var}(\hat{\mathbf{X}}_{\mathbf{signal}})}{\mathbf{Var}(\hat{\mathbf{X}}_{\mathbf{noise}})} \tag{18}$$

When homodyning is considered, backscattered light is received by a beamsplitter, where the incoming mode is mixed with the vacuum. Consequently, the numerator in (18) is rescaled according to the beamsplitter's transmission coefficient η, $\mathbf{Var}(\hat{\mathbf{X}}_{\mathbf{signal}}) = \eta^{\mathbf{2}}\mathbf{Var}(\hat{\mathbf{X}}_{\mathbf{signal}})$.
Note that the term $\mathbf{Var}(\hat{\mathbf{X}}_{\mathbf{signal}})$ involves only the signal produced at the transmitter (sender) and doesn't include any noise contributions. So by writing our TMSS as a squeezed vacuum, then utilizing the unitarity of the squeezing operator and the following Bogoliubov transformation,

$$\begin{aligned} \hat{\mathbf{a}}(\zeta) &= \cosh \mathbf{r}\ \hat{\mathbf{a}} + \mathbf{e}^{\mathbf{i}\phi} \sinh \mathbf{r}\ \hat{\mathbf{b}}^\dagger \\ \hat{\mathbf{b}}(\zeta) &= \cosh \mathbf{r}\ \hat{\mathbf{b}} + \mathbf{e}^{\mathbf{i}\phi} \sinh \mathbf{r}\ \hat{\mathbf{a}}^\dagger \end{aligned} \tag{19}$$

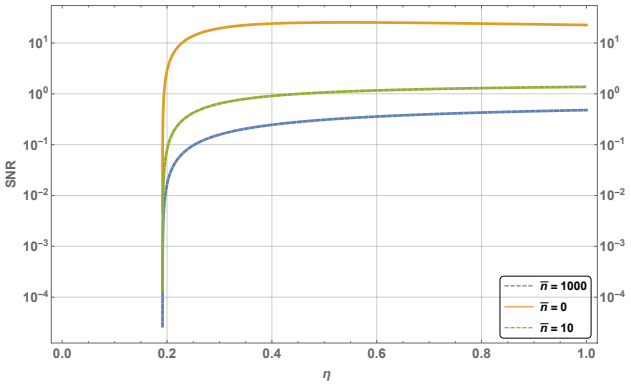

FIG. 5: *SNR in the case of homodyne detection plotted for different* $\bar{\mathbf{n}}$.

we get the following expression for the variance of the signal quadrature.

$$\mathbf{Var}(\hat{\mathbf{X}}_{\mathbf{signal}}) = \mathbf{1} + \mathbf{2}\ \sinh^{\mathbf{2}} \mathbf{r} \tag{20}$$

As for the denominator, after the beamsplitter it looks like

$$\mathbf{Var}(\hat{\mathbf{X}}_{\mathbf{noise}}) = \eta \mathbf{Var}(\hat{\mathbf{X}}_{\mathbf{input}}) + (\mathbf{1} - \eta)\mathbf{Var}(\hat{\mathbf{X}}_{\mathbf{vacuum}}) \tag{21}$$

where $\mathbf{Var}(\hat{\mathbf{X}}_{\mathbf{input}})$ is the variance of the input light beam after passing through either the thermal or the passive channel, while $\mathbf{Var}(\hat{\mathbf{X}}_{\mathbf{vacuum}})$ is the vacuum uncertainty, which in our case is normalized to $\mathbf{1}$. In either case, the expression for $\mathbf{Var}(\hat{\mathbf{X}}_{\mathbf{input}})$ can be imported directly from our previous calculation of the covariance matrix (see section II-C), where, for a thermal channel the input variance is,

$$\mathbf{Var}(\hat{\mathbf{X}}_{\mathbf{input}}) = (\mathbf{2}\ \mathbf{e}^{-\mathbf{2}\kappa \mathbf{t}} \sinh^{\mathbf{2}} \mathbf{r}) + \mathbf{1} + \bar{\mathbf{n}} \tag{22}$$

while in the case of a pure loss channel we have

$$\mathbf{Var}(\hat{\mathbf{X}}_{\mathbf{input}}) = (\mathbf{2}\ \mathbf{e}^{-\mathbf{2}\kappa \mathbf{t}} \sinh^{\mathbf{2}} \mathbf{r}) + \mathbf{1} \tag{23}$$

In Fig.5 we have plotted the SNR against the beamsplitter's transmission coefficient η. As can be seen, for the thermal environment the SNR is low and only reaches its maximum when η approaches 1. We can also note that the SNR degrades significantly as the number of noise photons $\bar{\mathbf{n}}$ increases. Conversely, for the case of a pure loss channel, the SNR is dramatically higher, since the environment adds no noise photons. Furthermore, as time progresses, i.e; when κt increases, the SNR can be enhanced further, since entanglement is always preserved (see Fig.4) and more signal reaches the detector. Another point worth mentioning is that the SNR for small values of η vanishes, this is mainly due to the process of homodyning itself, where in homodyne detection the weak input field is mixed with a strong local oscillator (LO) (a coherent state) on a low reflectivity beamsplitter, in order to avoid the risk of losing the input field in favour of the LO. In our case, mixing the input field with the vacuum gives exactly the same effect, since the variance of the vacuum is similar to that of a coherent state. Thus, small values of η are irrelevant and just contribute to plain noise.
For the sake of comparison, let us now consider direct detection of photons. We will investigate the variance of the photon number operator $\langle \Delta \hat{\mathbf{n}}^2 \rangle$ to determine how the expression in (17) behaves in different environments. For the pure loss channel,

the photon number variance of a TMSS is

$$\langle \Delta \hat{\mathbf{n}}^2 \rangle = \langle \hat{\mathbf{n}}^2 \rangle - \langle \hat{\mathbf{n}} \rangle^2 = \mathbf{e}^{-\mathbf{4}\kappa \mathbf{t}} \sinh^{\mathbf{2}} \mathbf{r} (\cosh^{\mathbf{2}} \mathbf{r} + \sinh^{\mathbf{2}} \mathbf{r}) \tag{24}$$

while for the thermal environment we have,

$$\begin{aligned} \langle \Delta \hat{\mathbf{n}}^2 \rangle = \mathbf{e}^{-\mathbf{4}\kappa \mathbf{t}} \sinh^{\mathbf{2}} \mathbf{r} (\cosh^{\mathbf{2}} \mathbf{r} + \sinh^{\mathbf{2}} \mathbf{r}) \\ + \mathbf{e}^{-\mathbf{4}\kappa \mathbf{t}} \bar{\mathbf{n}} (\sinh^{\mathbf{2}} \mathbf{r} + \cosh^{\mathbf{2}} \mathbf{r}) + \bar{\mathbf{n}}^{\mathbf{2}} \end{aligned} \tag{25}$$

In the previous equation, it can be noted that noise will dominate (25) as the bath temperature increases. Then by plugging in (25) into (17), we can see that the SNR ≈ 0. Thus, we can conclude that homodyne detection is more efficient in environments overwhelmed by thermal photons, while direct detection methods seem to be favourable inside cryogenic environments.

IV. Conclusion

In this paper, a new model for quantum backscatter communication (QBC) was proposed. Unlike previous QBC realizations, we have considered retaining the idler mode inside a lossy memory element, until a measurement is performed. After that, we investigated the effects of two different loss mechanisms on signal-idler correlations. Our analysis showed that when one of the modes traverses a thermal environment while the other propagates through a pure loss channel, the correlations between the two modes experience a phenomenon called "entanglement sudden-death". On the other hand, when both modes are subjected to pure loss, entanglement can always survive. We also examined briefly the received SNR according to two different detection methods. Our study showed that homodyne detection is preferable when thermal environments are considered. Finally, with advanced bath engineering techniques we think that QBC can be achieved inside thermal environments.

A. Appendix

1. Damping of backscattered signals in a thermal environment

In this appendix we outline briefly the dynamics of backscattered signals inside a thermal environment.
By assuming a large, unchanging environment (Born approximation), that is discrete and memoryless (Markov approximation) [18, 22], the master equation of a backscattered signal coupled to a heat bath can be written as

$$\begin{aligned} \frac{\mathbf{d}\hat{\rho}}{\mathbf{dt}} = \frac{\Upsilon}{2} (\bar{\mathbf{n}}(\omega_{\mathbf{0}}) + \mathbf{1}) [\mathbf{2}\hat{\mathbf{a}}\hat{\rho}\hat{\mathbf{a}}^\dagger - \hat{\mathbf{a}}^\dagger \hat{\mathbf{a}}\hat{\rho} - \hat{\rho}\hat{\mathbf{a}}^\dagger \hat{\mathbf{a}}] \\ + \frac{\Upsilon}{2} (\bar{\mathbf{n}}(\omega_{\mathbf{0}})) [\mathbf{2}\hat{\mathbf{a}}^\dagger \hat{\rho}\hat{\mathbf{a}} - \hat{\mathbf{a}}\hat{\mathbf{a}}^\dagger \hat{\rho} - \hat{\rho}\hat{\mathbf{a}}\hat{\mathbf{a}}^\dagger] \end{aligned} \tag{A1}$$

where $\bar{\mathbf{n}}(\omega_{\mathbf{0}})$ is the average number of blackbody photons as a function of the mode frequency, and "Υ" is the decay rate.
Afterwards, we use (A1) to derive the time dependence of the mode operator

$$\begin{aligned} \frac{\mathbf{d}\langle \hat{\mathbf{a}} \rangle}{\mathbf{dt}} = \frac{\mathbf{d}(\mathbf{Tr}(\hat{\mathbf{a}}\hat{\rho}))}{\mathbf{dt}} = \mathbf{Tr}(\hat{\mathbf{a}} \frac{\mathbf{d}\hat{\rho}}{\mathbf{dt}}) \\ = \frac{\Upsilon}{2} (\bar{\mathbf{n}}(\omega_{\mathbf{0}}) + \mathbf{1}) [\mathbf{2}\hat{\mathbf{a}}\hat{\mathbf{a}}\hat{\rho}\hat{\mathbf{a}}^\dagger - \hat{\mathbf{a}}\hat{\mathbf{a}}^\dagger \hat{\mathbf{a}}\hat{\rho} - \hat{\mathbf{a}}\hat{\rho}\hat{\mathbf{a}}^\dagger \hat{\mathbf{a}}] \\ + \frac{\Upsilon}{2} (\bar{\mathbf{n}}(\omega_{\mathbf{0}})) [\mathbf{2}\hat{\mathbf{a}}\hat{\mathbf{a}}^\dagger \hat{\rho}\hat{\mathbf{a}} - \hat{\mathbf{a}}\hat{\mathbf{a}}\hat{\mathbf{a}}^\dagger \hat{\rho} - \hat{\mathbf{a}}\hat{\rho}\hat{\mathbf{a}}\hat{\mathbf{a}}^\dagger] \end{aligned} \tag{A2}$$

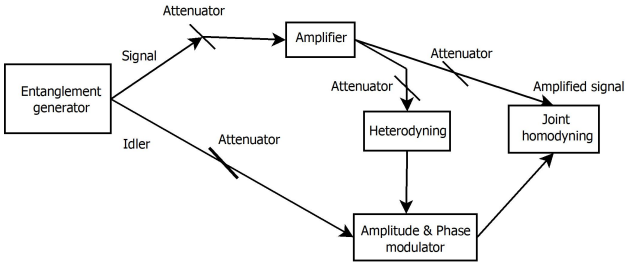

FIG. 6: *Avoiding entanglement sudden-death by utilizing an attenuator-amplifier chain.*

Then using the cyclic property of the trace yields,

$$\begin{aligned} = \frac{\Upsilon}{2} (\bar{\mathbf{n}}(\omega_{\mathbf{0}}) + \mathbf{1}) [\mathbf{2}\hat{\mathbf{a}}^\dagger \hat{\mathbf{a}}\hat{\mathbf{a}}\hat{\rho} - \hat{\mathbf{a}}\hat{\mathbf{a}}^\dagger \hat{\mathbf{a}}\hat{\rho} - \hat{\mathbf{a}}^\dagger \hat{\mathbf{a}}\hat{\mathbf{a}}\hat{\rho}] \\ + \frac{\Upsilon}{2} (\bar{\mathbf{n}}(\omega_{\mathbf{0}})) [\mathbf{2}\hat{\mathbf{a}}\hat{\mathbf{a}}\hat{\mathbf{a}}^\dagger \hat{\rho} - \hat{\mathbf{a}}\hat{\mathbf{a}}\hat{\mathbf{a}}^\dagger \hat{\rho} - \hat{\mathbf{a}}\hat{\mathbf{a}}^\dagger \hat{\mathbf{a}}\hat{\rho}] \end{aligned} \tag{A3}$$

After a little bit of bosonic algebra, i.e. $[\hat{\mathbf{a}}, \hat{\mathbf{a}}^\dagger] = \mathbf{1}$, we get,

$$\begin{aligned} \frac{\mathbf{d}\langle \hat{\mathbf{a}} \rangle}{\mathbf{dt}} = \frac{-\boldsymbol{\Upsilon}}{\mathbf{2}} \langle \hat{\mathbf{a}} \rangle, \\ \langle \hat{\mathbf{a}} \rangle = \mathbf{e}^{\frac{-\Upsilon \mathbf{t}}{\mathbf{2}}} \langle \hat{\mathbf{a}} \rangle \end{aligned} \tag{A4}$$

Consequently, the time derivative of the mode operator can be written as a decaying field plus a fluctuating noise term (known also as Langevin force) that has a vanishing mean value.

$$\begin{aligned} \hat{\mathbf{a}}_{\mathbf{out}} = \frac{\mathbf{d}\hat{\mathbf{a}}}{\mathbf{dt}} = \mathbf{e}^{\frac{-\Upsilon \mathbf{t}}{\mathbf{2}}} \hat{\mathbf{a}}_{\mathbf{in}} + \hat{\mathbf{N}} \\ \langle \hat{\mathbf{N}} \rangle = 0 \end{aligned} \tag{A5}$$

Equation (A5) is known as the quantum Langevin equation. As can be seen, it is written as a simple input-output relation plus a noise term, thus a quantum beamsplitter can accurately simulate this equation. Similar analysis is carried out to derive the dynamics of a mode operator inside a pure loss channel (a bath at zero temperature), however in such case we have to set $\bar{\mathbf{n}}$ to 0 in A1, and then proceed as in A2–A4

2. Avoiding entanglement sudden-death

As stated earlier in section II-C, the interaction between the signal mode and a severe thermal environment could lead to a phenomenon called entanglement sudden-death. Furthermore, coupling a cryogenic environment to a thermal bath is also not easy, since the injection of thermal noise into a cryostat would certainly damage the superconducting equipment that reside within. In this appendix we adapt a solution which is usually used in quantum optical networks [27], to protect our signal against entanglement sudden-death. As shown in Fig.6, the signal mode traverses a cascade of attenuator-amplifier elements. The attenuator (pure loss channel) is a two-port microwave network that can be engineered to have a specific cut-off frequency [28], such that, only the signal mode propagates through it, while the non-resonating noise modes are dissipated by resistive elements. Thus, a beamsplitter with the appropriate transmission coefficient can model this attenuator precisely. Building on this remark, we can now couple a cryogenic environment to a heat

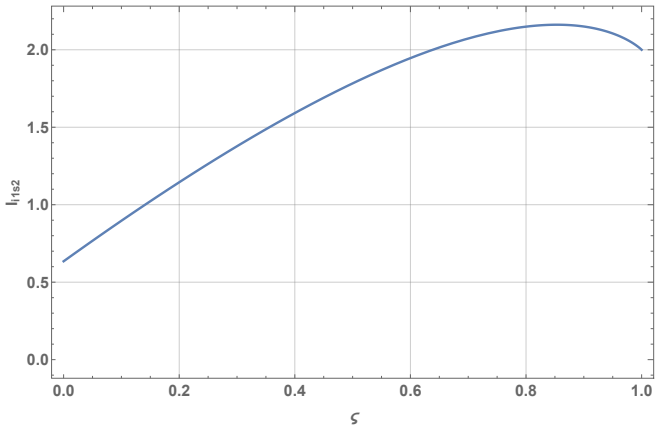

FIG. 7: *The inseparability criterion against the system losses [29]* .

bath without letting in a horde of noise photons. On the other hand, the role of the amplifier is to compensate for the loss caused by the attenuator. The amplifier design in Fig.6 follows that in [29], where it has been shown that entanglement can be preserved under the amplification method adopted. For our purposes, we are just concerned with the case where noise-reduced amplification can be performed within a tolerable loss, while the rest of the manuscript [29] deals also with other interesting cases. We will now turn our attention towards the protocol depicted in Fig.6. The entanglement generator generates entangled signal-idler pairs via the process of spontaneous down conversion, which can be expressed as

$$\begin{aligned} \hat{\mathbf{a}}_{\mathbf{s1}} &= \mathbf{G_1}\ \hat{\mathbf{a}}_{\mathbf{s0}} + \mathbf{g}_1\ \hat{\mathbf{a}}^{\dagger}_{\mathbf{i0}} \\ \hat{\mathbf{a}}_{\mathbf{i1}} &= \mathbf{G_1}\ \hat{\mathbf{a}}_{\mathbf{i0}} + \mathbf{g}_1\ \hat{\mathbf{a}}^{\dagger}_{\mathbf{s0}} \end{aligned} \tag{A6}$$

where $\mathbf{G_1}$ is the amplitude gain of the non-linear process, and $\mathbf{g_1^2 = G_1^2 - 1}$. Spontaneous down conversion can be, in some sense, thought of as an amplification process, where the vacuum signal and idler modes $\hat{\mathbf{a}}_{\mathbf{s0}}, \hat{\mathbf{a}}_{\mathbf{i0}}$ are the initial seeds of the amplifier, while $\hat{\mathbf{a}}_{\mathbf{s1}}, \hat{\mathbf{a}}_{\mathbf{i1}}$ are the amplifier's outputs. Furthermore, it can be noted that (A6) exactly resembles the Bogoliubov transformation in (19), since squeezing and spontaneous down conversion are equivalent to one another. Next, the signal mode traverses the attenuator-amplifier chain, while the idler propagates through a pure loss channel, as in the original model. For simplicity we will assume that the loss coefficients of the attenuators in Fig.6 are the same, thus

$$\hat{\mathbf{a}}^{\mathbf{out}}_{\mathbf{j}} = \sqrt{\mathbf{1-\varsigma}}\ \hat{\mathbf{a}}_{\mathbf{j}} + \sqrt{\varsigma}\ \hat{\mathbf{v}} \tag{A7}$$

where ς is the beamsplitter's reflection coefficient, $\mathbf{j = s1, i1}$, and $\hat{\mathbf{v}}$ is a vacuum mode. After that, the signal mode enters a parametric amplifier with a strong pump field. The input-output relations for the amplifier are given by

$$\begin{aligned} \hat{\mathbf{a}}_{\mathbf{s2}} &= \mathbf{G_2}\ \hat{\mathbf{a}}^{\mathbf{out}}_{\mathbf{s1}} + \mathbf{g}_2\ \hat{\mathbf{a}}^{\dagger}_{\mathbf{v0}} \\ \hat{\mathbf{a}}_{\mathbf{i2}} &= \mathbf{G_2}\ \hat{\mathbf{a}}_{\mathbf{v0}} + \mathbf{g}_2\ \hat{\mathbf{a}}^{\dagger\mathbf{out}}_{\mathbf{s1}} \end{aligned} \tag{A8}$$

where $\mathbf{G_2}$ is the amplitude gain of the amplifier, $\mathbf{g_2^2 = G_2^2 - 1}$, $\hat{\mathbf{a}}_{\mathbf{v0}}$ is the amplifier's noise mode and $\hat{\mathbf{a}}_{\mathbf{i2}}$ is a new mode generated by the parametric process to satisfy the energy conservation constraint. Similarly, the output modes $\hat{\mathbf{a}}_{\mathbf{s2}}$, $\hat{\mathbf{a}}_{\mathbf{i2}}$ are quantum correlated in the same way as $\hat{\mathbf{a}}_{\mathbf{s1}}$, $\hat{\mathbf{a}}_{\mathbf{i1}}$. For the sake of practicality, we will assume that the amplifier outputs are subjected to loss as described by (A7). To suppress the noise added by the amplifier $\hat{\mathbf{a}}_{\mathbf{v0}}$, the auxiliary mode $\hat{\mathbf{a}}_{\mathbf{i2}}$—which is quantum correlated with $\hat{\mathbf{a}}_{\mathbf{s2}}$— is heterodyned, and the resulting photo-currents are utilized to modulate $\hat{\mathbf{a}}_{\mathbf{i1}}$ in order to enhance the entanglement between the modes $\hat{\mathbf{a}}_{\mathbf{i1}}$ and $\hat{\mathbf{a}}_{\mathbf{s2}}$. The degree of entanglement or inseparability $\mathbf{I_{i1s2}}$ between $\hat{\mathbf{a}}_{\mathbf{i1}}$ and $\hat{\mathbf{a}}_{\mathbf{s2}}$ can be quantified by [2]

$$\mathbf{I_{i1s2}} = \langle \mathbf{\Delta \hat{X}^2_{-,i1s2}} \rangle + \langle \mathbf{\Delta \hat{P}^2_{+,i1s2}} \rangle \tag{A9}$$

where $\mathbf{\hat{X}_{-,i1s2} = (\hat{X}_{i1} - \hat{X}_{s2})/\sqrt{2}}$, $\mathbf{\hat{P}_{+,i1s2} = (\hat{P}_{i1} + \hat{P}_{s2})/\sqrt{2}}$, $\mathbf{\hat{X}_k = \hat{a}_k + \hat{a}^{\dagger}_k}$, $\mathbf{\hat{P}_k = i\ \hat{a}^{\dagger}_k - i\ \hat{a}_k}$, and $\mathbf{k = i1, s2}$
The modes $\hat{\mathbf{a}}_{\mathbf{i1}}$ and $\hat{\mathbf{a}}_{\mathbf{s2}}$ are said to be entangled (inseparable) only when $\mathbf{I_{i1s2} < 2}$. When the losses are maximum $\varsigma = 1$ the modes are replaced with the vacuum, such that, the uncertainty of the quadratures is equal to that of a vacuum state. Finally, after performing a joint quadrature measurement, we can plot the inseparability $\mathbf{I_{i1s2}}$ against the system losses ς. As can be seen in Fig.7 the inseparability condition is violated only when the losses exceed 0.64, which is still an impressive result, since all the modes involved were assumed to be lossy. To summarize, in this appendix we have proposed a solution based on [29] to avoid sudden-death of entanglement in quantum backscatter networks. Our model utilizes a cascade of attenuator-amplifier elements to couple a transmitter residing inside a cryostat to a thermal bath. The auxiliary mode generated during the amplification process—which is usually discarded— has been exploited to reduce the amplifier's noise. Finally, the proposed solution can also tolerate losses to some extent, thus it is suitable for practical applications.

3. Correlation matrix for the signal-idler pair

For illustration purposes, we calculate here the block element α of the covariance matrix. We recall that the matrix α is concerned with the idler mode variances,

$$\alpha = \frac{\mathbf{1}}{\mathbf{2}} \langle \hat{\mathbf{X}}_{\mathrm{m}} \hat{\mathbf{X}}_{\mathrm{j}} + \hat{\mathbf{X}}_{\mathrm{m}} \hat{\mathbf{X}}_{\mathrm{j}} \rangle_{\mathbf{TMSS}} - \langle \hat{\mathbf{X}}_{\mathrm{m}} \rangle_{\mathbf{TMSS}} \langle \hat{\mathbf{X}}_{\mathrm{j}} \rangle_{\mathbf{TMSS}} \tag{A10}$$

where $\mathbf{m, j = 1, 2}$, and $\mathbf{\hat{X}_1 = \frac{(\hat{a} + \hat{a}^{\dagger})}{\sqrt{2}}}$, $\mathbf{\hat{X}_2 = \frac{(\hat{a} - \hat{a}^{\dagger})}{i\sqrt{2}}}$
Then writing the TMSS as a squeezed vacuum implies,

$$\mathbf{\langle 0 |\, \hat{X}_{m,j}\, | 0 \rangle = 0} \tag{A11}$$

For the first quadrature we get

$$\begin{aligned} &\frac{\mathbf{1}}{\mathbf{2}} \mathbf{\langle 0, 0 |}\, \hat{\mathcal{S}}^{\dagger}(\zeta) (\mathbf{\Gamma \hat{a}_{in} + \hat{N} + \Gamma \hat{a}^{\dagger}_{in} + \hat{N}^{\dagger}}) \\ &\quad (\mathbf{\Gamma \hat{a}_{in} + \hat{N} + \Gamma \hat{a}^{\dagger}_{in} + \hat{N}^{\dagger}}) \hat{\mathcal{S}}(\zeta)\, \mathbf{| 0, 0 \rangle} \end{aligned} \tag{A12}$$

where we used (10).
By using the unitarity of the squeezing operator, the Bogoliubov transformation (19), and the noise properties in (11), we can now calculate second order moments like $\langle \mathbf{\hat{a}^2} \rangle, \langle \mathbf{\hat{a}^{\dagger 2}} \rangle, \langle \mathbf{\hat{a}\hat{N}} \rangle, \langle \mathbf{\hat{a}\hat{a}^{\dagger}} \rangle, \langle \mathbf{\hat{a}^{\dagger}\hat{a}} \rangle, \langle \mathbf{\hat{N}^{\dagger}\hat{N}} \rangle, \langle \mathbf{\hat{N}\hat{N}^{\dagger}} \rangle$. Similarly, we can calculate the other block elements.

[1] C. L. Degen, F. Reinhard, and P. Cappellaro, "Quantum sensing," *Rev. Mod. Phys.*, vol. 89, p. 035002, Jul 2017. [Online]. Available: https://link.aps.org/doi/10.1103/RevModPhys.89.035002

[2] R. Horodecki, P. Horodecki, M. Horodecki, and K. Horodecki, "Quantum entanglement," *Rev. Mod. Phys.*, vol. 81, pp. 865–942, Jun 2009. [Online]. Available: https://link.aps.org/doi/10.1103/RevModPhys.81.865

[3] C. H. Bennett, G. Brassard, and N. D. Mermin, "Quantum cryptography without Bell's theorem," *Phys. Rev. Lett.*, vol. 68, pp. 557–559, Feb 1992. [Online]. Available: https://link.aps.org/doi/10.1103/PhysRevLett.68.557

[4] A. K. Ekert, "Quantum cryptography based on Bell's theorem," *Phys. Rev. Lett.*, vol. 67, pp. 661–663, Aug 1991. [Online]. Available: https://link.aps.org/doi/10.1103/PhysRevLett.67.661

[5] S.-K. Liao, W.-Q. Cai, W.-Y. Liu, L. Zhang, Y. Li, J.-G. Ren, J. Yin, Q. Shen, Y. Cao, Z.-P. Li *et al.*, "Satellite-to-ground quantum key distribution," *Nature*, vol. 549, no. 7670, p. 43, 2017.

[6] Z. Wang, R. Malaney, and J. Green, "Inter-satellite quantum key distribution at terahertz frequencies," *arXiv preprint arXiv:1902.07921*, 2019.

[7] C. H. Bennett, G. Brassard, C. Crépeau, R. Jozsa, A. Peres, and W. K. Wootters, "Teleporting an unknown quantum state via dual classical and einstein-podolsky-rosen channels," *Phys. Rev. Lett.*, vol. 70, pp. 1895–1899, Mar 1993. [Online]. Available: https://link.aps.org/doi/10.1103/PhysRevLett.70.1895

[8] D. Bouwmeester, J.-W. Pan, K. Mattle, M. Eibl, H. Weinfurter, and A. Zeilinger, "Experimental quantum teleportation," *Nature*, vol. 390, no. 6660, p. 575, 1997.

[9] T. Ralph and A. Lund, "Nondeterministic noiseless linear amplification of quantum systems," in *AIP Conference Proceedings*, vol. 1110, no. 1. AIP, 2009, pp. 155–160.

[10] L.-M. Duan, M. Lukin, J. I. Cirac, and P. Zoller, "Long-distance quantum communication with atomic ensembles and linear optics," *Nature*, vol. 414, no. 6862, p. 413, 2001.

[11] M. Sanz, K. G. Fedorov, F. Deppe, and E. Solano, "Challenges in open-air microwave quantum communication and sensing," in *2018 IEEE Conference on Antenna Measurements & Applications (CAMA)*. IEEE, 2018, pp. 1–4.

[12] R. Di Candia, K. Fedorov, L. Zhong, S. Felicetti, E. Menzel, M. Sanz, F. Deppe, A. Marx, R. Gross, and E. Solano, "Quantum teleportation of propagating quantum microwaves," *EPJ Quantum Technology*, vol. 2, no. 1, p. 25, 2015.

[13] S. Lloyd, "Enhanced sensitivity of photodetection via quantum illumination," *Science*, vol. 321, no. 5895, pp. 1463–1465, 2008.

[14] S. Barzanjeh, S. Guha, C. Weedbrook, D. Vitali, J. H. Shapiro, and S. Pirandola, "Microwave quantum illumination," *Phys. Rev. Lett.*, vol. 114, p. 080503, Feb 2015. [Online]. Available: https://link.aps.org/doi/10.1103/PhysRevLett.114.080503

[15] R. Jäntti, R. Di Candia, R. Duan, and K. Ruttik, "Multiantenna quantum backscatter communications," in *2017 IEEE Globecom Workshops (GC Wkshps)*. IEEE, 2017, pp. 1–6.

[16] R. Di Candia, R. Jäntti, R. Duan, J. Lietzén, H. Khalifa, and K. Ruttik, "Quantum backscatter communication: A new paradigm," in *2018 15th International Symposium on Wireless Communication Systems (ISWCS)*. IEEE, 2018, pp. 1–6.

[17] H. Khalifa and R. Jäntti, "Quantum backscatter communication with photon number states," in *2018 IEEE Globecom Workshops (GC Wkshps)*. IEEE, 2018, pp. 1–6.

[18] J. Garrison and R. Chiao, *Quantum optics*. Oxford University Press, 2008.

[19] E. Knill, R. Laflamme, and G. J. Milburn, "A scheme for efficient quantum computation with linear optics," *nature*, vol. 409, no. 6816, p. 46, 2001.

[20] N. Hosseinidehaj, Z. Babar, R. Malaney, S. X. Ng, and L. Hanzo, "Satellite-based continuous-variable quantum communications: state-of-the-art and a predictive outlook," *IEEE Communications Surveys & Tutorials*, vol. 21, no. 1, pp. 881–919, 2018.

[21] Z. Shi, K. Dolgaleva, and R. W. Boyd, "Quantum noise properties of non-ideal optical amplifiers and attenuators," *Journal of Optics*, vol. 13, no. 12, p. 125201, 2011.

[22] G. S. Agarwal, *Quantum optics*. Cambridge University Press, 2012.

[23] T. Yu and J. Eberly, "Sudden death of entanglement," *Science*, vol. 323, no. 5914, pp. 598–601, 2009.

[24] A. Shabani and H. Neven, "Artificial quantum thermal bath: Engineering temperature for a many-body quantum system," *Physical Review A*, vol. 94, no. 5, p. 052301, 2016.

[25] H.-A. Bachor and T. C. Ralph, *A guide to experiments in quantum optics*. Wiley, 2004.

[26] R. W. Boyd, G. S. Agarwal, K. W. C. Chan, A. K. Jha, and M. N. OSullivan, "Propagation of quantum states of light through absorbing and amplifying media," *Optics Communications*, vol. 281, no. 14, pp. 3732–3738, 2008.

[27] E. Desurvire, "A three-dimensional quantum vacuum-noise/signal beamsplitter model for nonideal linear optical amplifiers," *Optical Fiber Technology*, vol. 5, no. 1, pp. 82–91, 1999.

[28] D. M. Pozar, *Microwave engineering*. John Wiley & Sons, 2009.

[29] J. Xin, X.-M. Lu, H. Wang, and J. Jing, "Preserving quantum entanglement from parametric amplifications with a correlation modulation scheme," *Physical Review A*, vol. 99, no. 1, p. 013813, 2019.